

# Learning an Optimally Reduced Formulation of OPF through Meta-optimization

Alex Robson, Mahdi Jamei, Cozmin Ududec, and Letif Mones

**Abstract**—We introduce a method for solving Optimal Power Flow (OPF) problems, which can substantially reduce solve times. A neural network that predicts the binding status of constraints of the system is used to generate an initial reduced OPF problem, defined by removing the predicted non-binding constraints. This reduced model is then extended in an iterative manner until guaranteeing an optimal solution to the full OPF problem. The classifier is trained using a meta-loss objective, defined by the total computational cost of solving the reduced OPF problems constructed during the iterative procedure. Using a wide range of DC- and AC-OPF problems we demonstrate that optimizing this meta-loss objective results in a classifier that significantly outperforms conventional loss functions used to train neural network classifiers. We also provide an extensive analysis of the investigated grids as well as an empirical limit of performance of machine learning techniques providing optimal OPF solutions.

**Index Terms**—AC-OPF, DC-OPF, Meta-optimization

## I. INTRODUCTION

A central task of electricity grid operators [1] is to frequently solve some form of Optimal Power Flow (OPF) [2], which is at its core a constrained optimization problem. The goal of OPF is to dispatch generation in order to meet demand at minimal cost, while respecting reliability and security constraints. This is a challenging problem for several reasons. First, OPF is a non-convex and non-linear constrained optimization problem that can take a mixed-integer form when solving the unit commitment problem. Second, it is computationally expensive due to the size of power grids, requiring a large number of diverse constraints to be satisfied. Further, grid operators must typically meet (at least)  $N-1$  reliability requirements (e.g. North American Electric Reliability Cooperation requirement for the US grid operators [3]), resulting in additional constraints that significantly increase the computational complexity of OPF. Finally, with increasing uncertainty in grid conditions due to the integration of renewable resources (such as wind and solar), OPF problems need to be solved near real-time to have the most accurate inputs reflecting the latest state of the system. This in turn requires the grid operators to have the computational capacity of running consecutive instances of OPF problems with fast convergence time.

OPF problems are typically solved through interior-point methods [4], also known as barrier methods (Figure 1, left panel). One of the most widely used approaches is the primal-dual interior-point technique with a filter line-search [5].

These methods are robust but expensive, as they require the computation of the second derivative of the Lagrangian at each iteration. Nevertheless, interior-point methods can be considered standard baseline approaches to solve general OPF problems.

In order to reduce computational costs, various approximations are used. The most typical approximation, called DC-OPF [2], makes the problem convex and reduces the number of variables and constraints. Black-box machine learning approaches are also being deployed to predict the solution of OPF, shifting computational effort away from real-time to offline training. These roughly fall into two categories.

One black-box approach is based on predicting the optimal OPF solution through regression techniques. Note that because OPF is a constrained optimization problem, the solution is not a smooth function of the grid parameters, so properly training such regression models requires substantial training data [6], [7]. There is also no guarantee that the solution satisfies all constraints, and violation of important constraints could lead to severe security issues for the grid. Nevertheless, the predicted solution can instead be utilized as a set-point to initialize an interior-point method (Figure 1, middle panel). This approach can significantly reduce the number of optimization iterations compared to the original problem [8], but the computational gain realized in practice is marginal for several reasons. First, because only primal variables are initialized, the duals still need to converge, as interior-point methods require a minimum number of iterations even if the primals are set to their optimal values. Trying to predict the duals as well makes the task even more challenging. Second, if the initial values of primals are far from optimal, the optimization can lead to a different local minimum. Finally, even if the predicted values are close to the optimal solution, the initialization can be located in a region that could result in substantially longer solve times, or even convergence failure.

The second black-box approach leverages the observation that only a fraction of constraints are actually binding at the optimum [9], so a reduced OPF problem can be formulated by keeping only the binding constraints. Since this reduced problem still has the same objective function as the original, the solution should be equivalent to that of the original full problem (Figure 1, right panel). This suggests a classification formulation, in which grid parameters are used to predict the binding status of each constraint [10], [11]. Unfortunately, this method can also lead to security issues through false negative predictions of the binding status of important constraints. However, by iteratively checking and adding violated constraints, and then solving the reduced OPF problem until all constraints of the full problem are satisfied, this issue can be avoided.

All authors are with Invenia Labs, 95 Regent Street, Cambridge, CB2 1AW, United Kingdom (e-mails: {firstname.lastname}@invenialabs.co.uk).

The authors thank Dr. Christian Steinruecken and Dr. Lyndon White for their suggestions that greatly improved the manuscript.

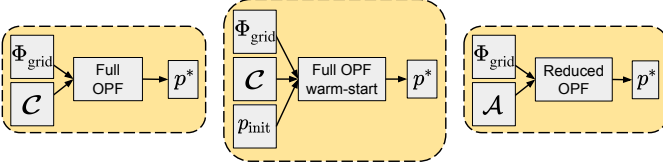


Fig. 1. OPF solution strategies for interior-point methods: direct (left), warm-start (middle), and reduced (right).  $\Phi_{\text{grid}}$  denotes the vector of grid parameters,  $\mathcal{C}$  and  $\mathcal{A}$  represent the full and active sets of constraints, respectively, and  $p^*$  and  $p_{\text{init}}$  are the optimal and initial values of the optimization variables.

As the reduced OPF problem is much cheaper than the full problem, this procedure (if converged in few iterations) can be very efficient.

This approach is compatible with current practices of some grid operators to solve OPF, where the transmission security constraints are enforced through an iterative procedure in which the solution at each iteration is checked against the base-case and  $N-1$  contingency constraints: all violated constraints are added to the model, and the procedure continues until no more violations are found [12]. We hereafter refer to this approach as the *iterative feasibility test*.

Focusing on the computational cost of obtaining a solution of the full OPF problem suggests the use of another loss function that measures this cost. In recent work we combined the regression approach with such an objective by minimizing the total number of the OPF solver iterations by predicting an appropriate warm-start for the interior-point primal variables [8]. We refer to this objective as a *meta-loss* and its optimization as *meta-optimization* – expressing the fact that we tune the parameters of the OPF optimization via a predictor.

Inspired by recent work in predicting active constraint sets [10], [11], [13], the main contribution of this paper is to combine the classifier approach with meta-optimization, to obtain a reduced OPF model where the computational cost of the iterative feasibility test is minimized. We demonstrate the capability of our method on several DC- and AC-OPF problems. To understand the theoretical limits of each approach, we explore a perfect regressor and classifier, as guides for further research in this direction. To understand the scalability of this method, a wide range of grid sizes are tested, some of which have not been explored before due to computational cost.

In order to facilitate research reproducibility in the field, we have made the generated DC- and AC-OPF samples publicly available (<https://github.com/invenia/OPFSampler.jl>).

## II. METHODS

### A. Meta-optimization for Regression

To introduce the concept of a meta-loss as an alternative objective function, we briefly describe a previous regression-based model [8].

Conventional supervised regression techniques typically use loss functions based on a distance between the training ground-truth and predicted output value, such as mean squared error or mean absolute error [14]. In general, each dimension of the target variable is treated equally in the loss function. However, the shape of the Lagrangian landscape of the OPF problem [15]

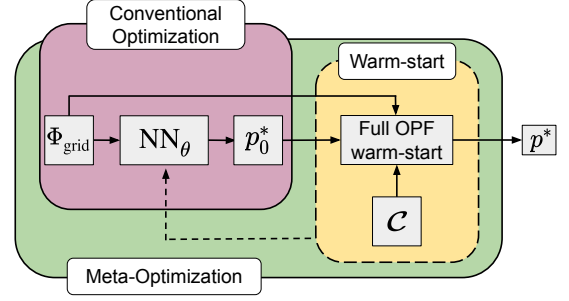


Fig. 2. Flowchart of the meta-optimization procedure using a NN regressor with warm-start. The initial values of weights  $\theta$  for meta-optimization of the meta-loss are obtained from conventional training with a regression loss.  $\Phi_{\text{grid}}$  is the vector of grid parameters,  $\text{NN}_\theta$  represents the regressor with weights  $\theta$ . The meta-loss is computed as the total number of optimization steps of the warm-started OPF.  $p_0^*$  is the initial value of the optimization variables and  $\mathcal{C}$  denotes the full set of constraints of the problem.

as a function of the optimization variables is far from isotropic, implying that optimization under such an objective does not necessarily minimize the warm-started OPF solution time.

Instead, we proposed a meta-loss function that directly measures the computational cost of solving the OPF problem. As the number of OPF optimization steps is roughly proportional to the solve time, the meta-loss function is defined to be the number of iterations of the interior-point method required to reach the optimal solution from the starting point, as predicted by the regression model. We applied a neural network (NN), with parameters determined by minimizing the meta-loss function (meta-optimization) on the training set (Figure 2). As this meta-loss is a non-differentiable function with respect to the NN weights, back-propagation cannot be used. As an alternative, we employed the Particle Swarm Optimization (PSO) [16], a gradient-free optimization method.

Meta-optimization requires solving OPF multiple times (as the predictor changes) and is therefore computationally demanding: with  $N_t$  meta-training samples,  $N_p$  PSO particles and  $N_s$  meta-optimization steps,  $N_t \times N_p \times N_s$  full OPF problems with warm-start must be solved. However, it is straightforward to start the meta-optimization from a pre-trained NN, under a conventional regression loss. We demonstrated the capability of this meta-optimization for two synthetic grids using DC-OPF problems [8].

### B. Meta-optimization for Classification

The first step of our new method is to train a NN-based classifier using grid parameters as features, to predict the binding status of the constraints of the full OPF problem. A reduced OPF problem has the same objective function as the full problem, but only retains those constraints that were predicted to be binding by the classifier. As there may be violated constraints not included in the reduced model, we use the *iterative feasibility test* to ensure convergence to an optimal solution of the full problem. The procedure has the following steps (Figure 3):

- 1) An initial reduced set of constraints  $\mathcal{A}_1$  is proposed by the classifier. A solution  $p_1^*$  is then obtained by solving the reduced problem.

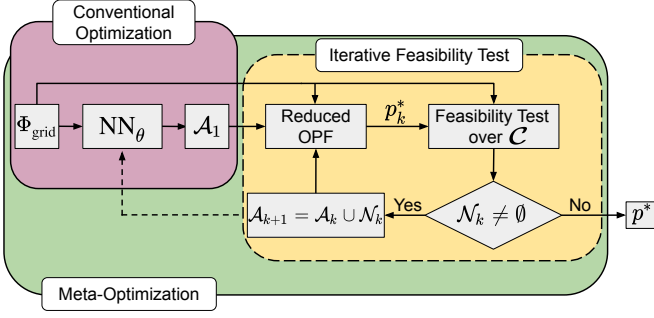


Fig. 3. Flowchart of the meta-optimization using an NN classifier under the feasibility iteration procedure. Conventional optimization of a classification loss, which provides initial weights  $\theta$ , is followed by a meta-optimization of the meta-loss.  $\Phi_{grid}$  is the vector of grid parameters,  $NN_\theta$  represents the classifier with weights  $\theta$ . The meta-loss is computed within the iterative feasibility test, where  $\mathcal{C}$  denotes the full set of constraints of the original OPF problem,  $\mathcal{A}_k$  is the actual set used in the reduced problem and  $\mathcal{N}_k$  is the set of violated constraints.  $p_k^*$  is the solution of the corresponding reduced problem, where  $k = 1 \dots K$  is the iteration index. The final solution  $p_K^* = p^*$  at  $k = K$  is obtained when  $\mathcal{N}_K = \emptyset$ .

- 2) In each feasibility iteration,  $k \in 1 \dots K$ , the solution  $p_k^*$  of the reduced problem is validated against the constraints  $\mathcal{C}$  of the original full formulation.
- 3) At each step  $k$ , the violated constraints  $\mathcal{N}_k$  are added to the set of considered constraints to form  $\mathcal{A}_{k+1} = \mathcal{A}_k \cup \mathcal{N}_k$ .
- 4) This procedure repeats until no violations are found (i.e.  $\mathcal{N}_K = \emptyset$ ), and the solution  $p_K^*$  satisfies all original constraints  $\mathcal{C}$ . At this point, we have found a solution to the full problem ( $p^*$ ).

We define the meta-loss objective as the total computation time of the iterative feasibility test procedure, and the meta-optimization as the optimization of the NN weights under the meta-loss objective over a training data set.

The meta-loss objective therefore includes the solution time of a sequence of reduced OPF problems. Similarly to the meta-loss defined for the regression approach, it measures the computational cost of obtaining a solution of the full problem. As the meta-loss is a non-differentiable function of the classifier weights, we optimize it using the gradient-free PSO method. The meta-optimization has the following computational cost: with  $N_t$  meta-training examples,  $N_p$  particles, and  $N_s$  meta-optimization steps,  $\sum_{i=1}^N K_i$  reduced OPF calculations are performed, where  $N = N_t \times N_p \times N_s$ , and  $K_i$  is the number of feasibility test iterations of the  $i$ th reduced OPF problem.

Of all these parameters,  $N_t$ ,  $N_p$  and  $N_s$  are the hyper-parameters we control. The values  $\{K_i\}_{i=1}^N$ , however, are dependent upon the classifier performance. In our experience, the procedure usually converges within a few iterations to the full solution (typically 1–10 for tested grids). We further note that instead of just extending the previous set of active constraints with violations, an alternative to step 3 would be to also discard constraints that were found to be non-binding in  $\mathcal{A}_k$ . This alternative approach can theoretically lead to infinite loops when competing constraints switch their binding status from one to another between consecutive iterations. We also found it to converge more slowly in practice than the extension-

only version we recommend in step 3.

To reduce the required number of steps of meta-optimization, we initialize the NN classifier by training under a conventional objective for classification. As discussed previously for regression, optimizing such an objective does not necessarily minimize the computational cost of obtaining a solution of the full problem. In practice, we achieve reasonable results by training with a cheap surrogate objective (conventional loss) first, followed by training under the more expensive meta-loss objective. We summarize the differences between regression and classification approaches in Table I.

TABLE I  
COMPARISON OF REGRESSION AND CLASSIFICATION APPROACHES USING META-OPTIMIZATION.

| Property                  | Regression                      | Classification                               |
|---------------------------|---------------------------------|--|
| Input                     | $\Phi_{grid}$                   | $\Phi_{grid}$                                |
| Output                    | $p_0^*$                         | $\mathcal{A}_1$                              |
| OPF problem type to solve | full OPF with warm-start        | reduced OPF formulations                     |
| Meta-loss                 | $n_{full-OPF} - n_{warm-start}$ | $\sum_{k=1}^K t_k^{reduced-OPF}$             |
| Meta-optimizer            | PSO varying NN weights          | PSO varying NN weights                       |
| Cost of meta-optimization | $N_t \times N_p \times N_s$     | $\sum_{i=1}^{N_t \times N_p \times N_s} K_i$ |

### C. OPF Framework

Several synthetic grids from the Power Grid Library [17] were used. DC- and AC-OPF models were solved within the PowerModels.jl [18] OPF package written in Julia [19]. For interior-point methods, Ipopt [5] was primarily used, with further comparisons to the ECOS [20] and OSQP [21] solvers.

### D. Input Sample Generation

In order to explore a variety of distinct active sets of constraints for the synthetic cases and mimic the time-varying behavior of the OPF input parameters, grid parameter samples with feasible OPF solutions were generated by varying the original values in the grid data-set. In particular, for each grid 10k DC-OPF samples were produced by re-scaling nodal load active power by factors drawn from uniform distribution of the form  $\mathcal{U}(0.85, 1.15)$ , and re-scaling maximum active power output of generators, line thermal ratings and line reactance values by scaling factors drawn from  $\mathcal{U}(0.9, 1.1)$ . For AC-OPF, 1k samples were generated for the studied synthetic grids. Beside the parameters that were changed for DC-OPF, re-scaled nodal load reactive power, maximum reactive power output of generators, and line resistance values were produced by scaling factors sampled from  $\mathcal{U}(0.9, 1.1)$ .

### E. Technical Details of the Model

1) *NN Architecture*: Each constraint was predicted to be binding or non-binding by a multi-label classifier. Correspondingly, a binary cross-entropy loss was used with the following architecture, in the Julia Flux.jl package [22]. Two fully connected hidden layers were each followed by a BatchNorm layer [23] and a ReLU activation function [24]. A Dropout layer [25] with a dropout fraction of 0.4 was added after

each BatchNorm layer. The final output layer had a sigmoid activation function. The input and output sizes of the NN were determined by the number of grid parameters, and the cardinality of all inequality constraints, respectively (see Tables II and III for details), while the middle layer size was  $50 \times 50$ .

2) *Conventional Optimization*: Samples were split randomly into training, validation, and testing sets of 70%, 20% and 10%, respectively. Hereafter, when referring to 10k or 1k samples, we refer to the total data set split as such. Mini-batch sizes of 10 and 100 were used with 1k and 10k samples, respectively. Training was carried out using the ADAM optimizer [26] (with learning-rate  $\eta = 10^{-4}$  and parameters  $\beta_1 = 0.9$  and  $\beta_2 = 0.999$ ), using early stopping with a patience of 10 determined on a validation set after a 50 epoch burn-in period.

3) *Binding Status of Constraints*: As the power flow equality constraints are always binding, we limited binding-state prediction to inequality constraints only. The binding status of generator output power lower-bound constraints was not predicted (but force-set to be always binding) as the reduced OPF problem may become unbounded with their removal. For similar optimization stability reasons, for AC-OPF the binding status of lower and upper bound limits of voltage magnitudes were not predicted either, and always set to binding. The binding status of the constraints was assigned by checking each side of the inequality constraints. We considered a constraint binding if either it was violated or the absolute value of the difference between the two sides was less than a fixed threshold value set at  $10^{-5}$ .

4) *Meta-optimization*: During meta-optimization, the NN weights obtained from conventional optimization were further varied to optimize the meta-loss objective, defined as the total computational time to solve each OPF problem in the meta-training data. At each evaluation, meta-training data was randomly sub-sampled from the training data with  $N_t = 100$ . For each investigated grid, 10 particles and 50 iterations of PSO were run, using the Optim.jl package [27]. The package was slightly modified to improve the particle initialization. The starting position of the particles in the NN weight space was derived from the weights of the conventionally optimized NN and each component was perturbed by a random number drawn from a normal distribution with zero mean and standard deviation set at the absolute value of the component.

Finally, in order to avoid converging to trivial minima of the meta-loss (discussed in Section-III-E) a penalty term was introduced during meta-optimization: if the number of predicted active constraints was higher than the twice the average number of the active constraints in the training data, the value of the meta-loss function was set to infinity.

### III. RESULTS

#### A. Distinct Active Sets in DC- and AC-OPF Samples

Based on the generated samples, we first investigated the number of unique active sets (congestion regimes) of several synthetic grids. Table II shows the results for DC-OPF samples with 10k and a random 1k subset. It also provides the number of grid parameters  $\dim(\Phi_{\text{grid}})$  (i.e., the classifier input size), the

TABLE II  
GRID CHARACTERISTICS AND NUMBER OF UNIQUE ACTIVE SETS FOR DIFFERENT DC-OPF CASES, USING 1K AND 10K SAMPLES.

| Case         | $\dim(\Phi_{\text{grid}})$ | $ \mathcal{C}_{\text{ineq}} $ | $ \mathcal{C}_{\text{eq}} $ | # active sets |           |       |
|--------------|----------------------------|-------------------------------|-----------------------------|---------------|-----------|-------|
|              |                            |                               |                             | Ref [13]      | This work |       |
|              |                            |                               |                             |               | 1k        | 10k   |
| 24-ieee-rtts | 125                        | 208                           | 63                          | 5             | 15        | 18    |
| 30-ieee      | 105                        | 168                           | 72                          | 1             | 1         | 1     |
| 39-epri      | 123                        | 204                           | 86                          | 2             | 8         | 12    |
| 57-ieee      | 206                        | 324                           | 138                         | 3             | 8         | 9     |
| 73-ieee-rtts | 387                        | 648                           | 194                         | 21            | 8         | 48    |
| 118-ieee     | 490                        | 768                           | 305                         | 2             | 66        | 122   |
| 162-ieee-dtc | 693                        | 1152                          | 447                         | 9             | 188       | 513   |
| 300-ieee     | 1080                       | 1754                          | 712                         | 22            | 835       | 5145  |
| 588-sdet     | 1846                       | 2916                          | 1275                        | —             | 826       | 5004  |
| 1354-pegase  | 4915                       | 7922                          | 3346                        | —             | 997       | 9506  |
| 2853-sdet    | 10275                      | 16750                         | 6775                        | —             | 1000      | 10000 |
| 4661-sdet    | 15401                      | 24944                         | 10659                       | —             | 1000      | 10000 |
| 9241-pegase  | 38438                      | 63402                         | 25291                       | —             | 1000      | 10000 |

number of inequality constraints ( $|\mathcal{C}_{\text{ineq}}|$ ), where the binding status is predicted (the classifier output size) and also the number of equality constraints ( $|\mathcal{C}_{\text{eq}}|$ ) that are always binding.

For the 1k subset, we compared the number of distinct active sets to those reported in [13], which were generated by scaling nodal load with a factor drawn from a normal distribution with  $\mu = 1.0$  and  $\sigma = 0.03$ . In the data presented here, the number of unique active sets is generally significantly higher that can be attributed to two major intentional differences: 1) varying more parameters beyond load, and 2) selecting a wider deviation for the load scaling values.

It is also clear from this setup that a sample size of 1k is too limited to cover all possible distinct active sets for these grids. When extending the number of samples to 10k we observe a further increase in the number of active sets. For larger grids, this is capped at the number of samples. This indicates that under the sampling distribution of grid parameters, convergence to the real distribution of active-sets becomes increasingly poor particularly for the larger grids with realistic sampling numbers.

We performed a similar analysis of grid properties for AC-OPF cases using 1k samples (Table III). As expected, the number of grid parameters and number of constraints are significantly higher than those of the corresponding DC-OPF cases. In Table III we split the number of equality constraints—that are always binding—into two sets: convex and non-convex. The number of convex equality constraints ( $|\mathcal{C}_{\text{eq}}^{\text{cvx}}|$ ) is very similar to those of DC-OPF, but there is also a great number of the non-convex equality constraints ( $|\mathcal{C}_{\text{eq}}^{\text{non-cvx}}|$ ). We note that the computation of the non-convex equality constraints and their first and second derivatives is the most expensive part of an interior-point optimization. Given that the systems are larger, it is not surprising that the number of distinct active sets is higher than those of the corresponding DC-OPF cases.

#### B. Maximum Achievable Gains

To compare the utility of a regression or classification approach, we begin with the estimation of the expected empirical limit of the achievable computational gain for different solvers. In practice, this is equivalent to computing the gain of computational cost of the perfect regressor or

TABLE III  
GRID CHARACTERISTICS AND NUMBER OF UNIQUE ACTIVE SETS FOR  
DIFFERENT AC-OPF CASES, USING 1K SAMPLES.

| Case         | $\dim(\Phi_{\text{grid}})$ | $ C_{\text{ineq}} $ | $ C_{\text{eq}}^{\text{cvx}} $ | $ C_{\text{eq}}^{\text{non-cvx}} $ | # active sets (1k) |
|--------------|----------------------------|---------------------|--------------------------------|------------------------------------|--------------------|
| 24-ieee-rtts | 214                        | 628                 | 49                             | 152                                | 39                 |
| 30-ieee      | 177                        | 576                 | 61                             | 164                                | 8                  |
| 39-epri      | 200                        | 670                 | 79                             | 184                                | 154                |
| 57-ieee      | 338                        | 1098                | 115                            | 320                                | 7                  |
| 73-ieee-rtts | 660                        | 1958                | 147                            | 480                                | 523                |
| 118-ieee     | 864                        | 2670                | 237                            | 744                                | 799                |
| 162-ieee-dtc | 1102                       | 3772                | 325                            | 1136                               | 812                |
| 300-ieee     | 1773                       | 5804                | 601                            | 1644                               | 1000               |
| 588-sdet     | 3006                       | 9770                | 1177                           | 2744                               | 1000               |
| 1354-pegase  | 7839                       | 27078               | 2709                           | 7964                               | 1000               |
| 2853-sdet    | 16629                      | 55462               | 5707                           | 15684                              | 1000               |

classifier: performing a warm-start OPF calculation using the value of the primal variables at the solution for the former and performing a reduced OPF problem with the exact set of binding constraints for the latter. Therefore, we computed the average maximum achievable gain for several grids using DC- and AC-OPF formulations with 1k samples. We define the gain of the computational cost to the full OPF problem as:

$$G(t_{\text{ML}}) = 100 \frac{t_f - t_{\text{ML}}}{t_f} \quad (1)$$

where  $t_f$  and  $t_{\text{ML}}$  are the computational times (or meta-losses) of the original full OPF problem and the machine-learning based approach, respectively. Here, we evaluate the average of  $G(t_{\text{ML}}^*) \geq G(t_{\text{ML}})$ , where  $t_{\text{ML}}^*$  is the computational time (meta-loss) of the corresponding perfect predictors.

Among the interior-point solvers used, only Ipopt had warm-start capability for the primal variables and therefore the maximum achievable gain for regression was investigated only for this solver, where the value of its `bound_push` and `bound_frac` parameters were set to  $10^{-9}$ . For DC-OPF classification, besides Ipopt, we also computed the maximal gain using two other (convex) solvers: ECOS and OSQP. For each sample we compared the optimal value of the objective of the warm-start and reduced OPF formulations to the solution of the full problem and found that they were indeed equal. This was especially necessary for AC-OPF cases, where finding the same solution is less evident due to the non-convex nature of the problem.

Table IV presents the results for both formulations. In the case of the DC formulation, for Ipopt we observe that the maximum achievable gain of the regression approach is in general somewhat lower than that of the classification approach, especially for larger grids. Further, while the maximal gain for regression shows little correlation with the grid size, there is a much stronger correlation for classification, indicating a better scaling when moving to larger grids.

For classification, the other two solvers show slightly better performance on the gain, though the correlation with the grid size is less strong. We also note that OSQP resulted in the highest maximum achievable gain among the investigated solvers. Given the DC-OPF is a linear problem we can draw some qualitative conclusions regarding the system size and gain. In the case of perfect regression the size of the optimization problem is equal to the original OPF problem and the gain is

determined by the convergence of dual variables that does not seem to depend on the size. However, the gain of a perfect classifier is primarily governed by the size of the reduced OPF problem compared to the full problem and it roughly depends on the ratio of the number of inequality constraints and number of all constraints of the full OPF formulation (assuming that only a fraction of inequality constraints are actually active).

TABLE IV  
MAXIMUM ACHIEVABLE GAINS OF WARM-START WITH PRIMAL VARIABLES  
(PERFECT REGRESSION) AND REDUCED OPF FORMULATIONS (PERFECT  
CLASSIFICATION) METHODS FOR SEVERAL GRIDS USING DC- AND AC-OPF  
FORMULATIONS.

| Case         | DC Gain (%) |            |                |            | AC Gain (%) |                |
|--------------|-------------|------------|----------------|------------|-------------|----------------|
|              | Regression  |            | Classification |            | Regression  | Classification |
|              | Ipopt       | Ipopt      | ECOS           | OSQP       | Ipopt       | Ipopt          |
| 24-ieee-rtts | 30.9 ± 0.7  | 29.9 ± 0.7 | 33.7 ± 0.6     | 57.2 ± 0.7 | 27.0 ± 0.6  | 25.2 ± 0.6     |
| 30-ieee      | 33.9 ± 0.5  | 28.3 ± 0.5 | 55.4 ± 0.5     | 56.6 ± 1.0 | 7.9 ± 0.8   | 32.0 ± 0.9     |
| 39-epri      | 52.7 ± 0.4  | 28.0 ± 0.4 | 46.4 ± 0.6     | 75.6 ± 1.5 | 46.0 ± 0.6  | 29.7 ± 0.6     |
| 57-ieee      | 27.1 ± 0.6  | 38.8 ± 0.3 | 54.2 ± 0.4     | 59.5 ± 1.0 | 21.4 ± 0.7  | 30.6 ± 0.7     |
| 73-ieee-rtts | 29.7 ± 0.3  | 36.8 ± 0.3 | 33.7 ± 0.4     | 64.8 ± 0.4 | 33.5 ± 0.7  | 27.6 ± 0.5     |
| 118-ieee     | 22.4 ± 0.5  | 47.6 ± 0.4 | 59.5 ± 0.3     | 54.4 ± 1.8 | 15.8 ± 0.6  | 31.1 ± 0.4     |
| 162-ieee-dtc | 55.4 ± 0.4  | 47.3 ± 0.3 | 56.6 ± 1.0     | 55.5 ± 1.9 | 40.4 ± 1.0  | 21.9 ± 0.7     |
| 300-ieee     | 44.1 ± 0.4  | 45.7 ± 0.3 | 52.2 ± 0.5     | 53.0 ± 1.6 | 37.2 ± 1.4  | 17.4 ± 0.6     |
| 588-sdet     | 28.5 ± 0.5  | 57.0 ± 0.3 | 57.4 ± 0.5     | 66.6 ± 0.7 | -18.3 ± 1.0 | 12.2 ± 0.8     |
| 1354-pegase  | 47.6 ± 0.4  | 47.0 ± 0.4 | 50.5 ± 0.6     | 42.8 ± 1.2 | 1.6 ± 1.3   | 35.1 ± 0.4     |
| 2853-sdet    | 34.8 ± 0.3  | 54.6 ± 0.2 | 49.5 ± 1.3     | 64.0 ± 0.6 | -9.9 ± 0.5  | 27.4 ± 0.3     |
| 4661-sdet    | 38.0 ± 0.3  | 45.1 ± 0.3 | 46.6 ± 1.4     | 63.2 ± 1.3 | —           | —              |
| 9241-pegase  | 40.2 ± 0.6  | 52.7 ± 0.6 | 48.0 ± 5.7     | 63.5 ± 0.9 | —           | —              |

For AC-OPF we found that the maximum achievable gain is more moderate for both regression and classification compared to those of DC-OPF. With the AC-OPF formulation, the gain of the perfect regression did not show a correlation with the system size, and for some cases we observed even negative gain with the warm-start OPF. Unlike the DC-OPF case, the gain of the perfect classification cannot be related simply to the ratio of inequality and equality constraints anymore: the computationally most expensive part is the calculation of the first and second derivatives of the non-convex equality constraints that are always binding (see Table III). In conclusion, we found that for DC-OPF the maximum achievable gain is significantly larger for classification ( $\approx 50\%$ ) than for regression (at least for larger grid sizes). No correlation was found between the system size and the gain of perfect regression, while a weak correlation was observed between the grid size and the gain of perfect classification. For AC-OPF, the maximum achievable gains are significantly lower than those for DC-OPF but for larger grids classification can still provide some improvement. We note that although the OSQP solver provided the highest gains of perfect classification for most of the grids, we still used Ipopt in the rest of this work to be consistent between AC and DC formulations and for other practical considerations.

### C. Meta-loss as a Function of False Negative and False Positive Predictions

We extended the empirical investigations away from perfect performance and examined the asymmetric effect of error in binding-constraint classification. Specifically, we investigated the effect of increasing false negative (i.e. binding constraints missing in the reduced formulation) and false positive (i.e. non-binding constraints predicted as binding) predictions on the meta-loss. We demonstrate our findings on grids 162-ieee-dtc



and 300-ieee with both DC and AC formulations using their default grid parameters. First, we solved the full OPF models and determined the binding constraints. To investigate the effect of false negative predictions we randomly removed one, two, three, etc., binding inequality constraints from the active set and computed the meta-loss. For false positive predictions we extended the active set by a given number of randomly selected constraints from the non-binding set.

For each case we ran 20 independent experiments and the results are presented in Figure 4. The left panel shows the actual meta-loss values, while the right panel presents the number of required iterations in the iterative feasibility test. For all cases vertical dashed lines indicate the position of the perfect classification, i.e. the exact active set when no false positive or false negative predictions are present. When all active constraints are found, including false positive constraints (moving right from the perfect classification) has a marginal effect, however, they slowly but surely increase the computational cost. The iterative feasibility test converges always within a single step and the cost of the OPF problem depends only on its size. False negative predictions (moving left from the perfect classification) have much more severe effect: they require more iterations in the feasibility test that significantly increases meta-loss even in the lack of few active constraints. Since for small grids the computational cost of the perfect prediction is only  $\sim 50\%$  of the full problem (Table IV) even a few iterations can have a meta-loss exceeding that of the full OPF problem. In all cases, different constraints represented (or removed) can have a different impact on the meta-loss, particularly in the false negative region where the deviation is larger.

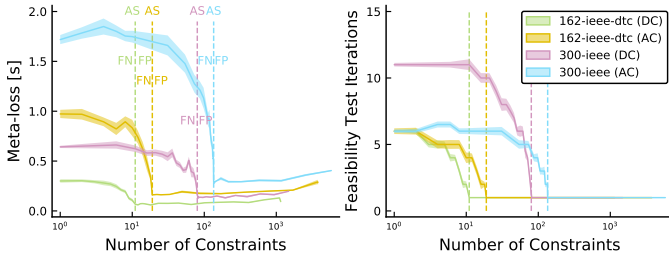


Fig. 4. Profile of the meta-loss (left) and number of iterations within the iterative feasibility test (right) as functions of the number of constraints for two grids, and a comparison of DC vs AC formulations. Perfect classifiers with the active set (AS) are indicated by vertical dashed lines, false positive (FP) region is to the right and false negative (FN) region is to the left.

#### D. Loss and Meta-loss During Conventional Optimization

To demonstrate that conventional loss optimization is not necessarily able to improve the meta-loss, we performed the following experiment on a smaller (73-ieee-rtts), and a larger (162-ieee-dtc) grid with DC-OPF formulations using the standard grid parameters on 1k samples. During the optimization of cross-entropy, we saved the actual NN weights every 5 epochs and computed both the loss and meta-loss values on the test set. The results are collected in Figure 5. For the smaller grid, which has only 8 distinct active sets in the training data (see Table II), the meta-loss also decreases

progressively due to a near-perfect performance of the classifier for such a simple system. However, for the larger 162-ieee-dtc grid the meta-loss seems to be insensitive to the optimization of the conventional loss.

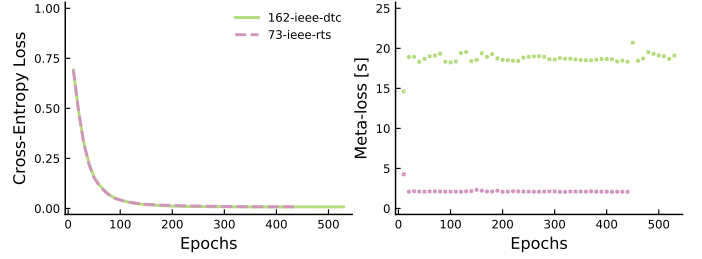


Fig. 5. Loss and meta-loss as functions of epochs during the optimization of the binary cross-entropy objective for a smaller (73-ieee-rtts) and a larger (162-ieee-dtc) grid.

#### E. Improving the Meta-loss using Meta-optimization

Finally, we present our results of the meta-optimization using 10k and 1k samples. We first carried out a conventional optimization of the cross-entropy loss and starting from this parameterization of the NN we further optimized the meta-loss through PSO. We computed the accumulated meta-loss of a test set before (pre) and after (post) the meta-optimization and computed the gain in the meta-loss relative to the full OPF problem in each case.

First we review the results for the DC-OPF formulation. For smaller grids up to grid 73-ieee-rtts we found marginal improvement using meta-optimization. The reason is similar to what we found in Section III-D: for such small systems with a limited number of distinct active sets (Table II) the classifiers were able to predict binding constraints almost perfectly and the meta-loss was already close to optimal.

For larger systems (from 118-ieee up to 1354-pegase) meta-optimization significantly improved the meta-loss. However, in many cases, we observed two trivial local minima the meta-optimization could converge to. The first trivial (Type 1) minimum mostly occurred with smaller training data and the classifier predicted most of the inequality constraints binding. This is a consequence of the fact that adding false positive predictions to the genuine active set only marginally increases the computational cost as it requires a single feasibility test iteration (Figure 4). This results in little signal (via the meta-loss) driving optimization away from prediction of all constraints binding to the active set. The second trivial (Type 2) minimum was observed with larger training data, and in this case the classifier essentially memorized all potentially active constraints in the training set. Both are the results of a classifier that has little discriminative power as in each case there is little sensitivity to the actual grid parameters with the optimization learning to allow only a single iteration of iterative feasibility test. Recalling that the maximum achievable gain of the grids we investigated is around 50% (Table IV), this means that even a single false negative prediction requires an extra iteration of the feasibility test, increasing the total computational time in comparison to the full problem. For

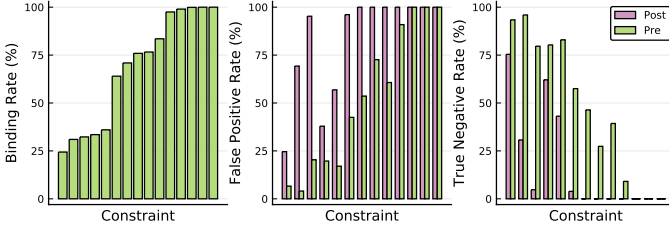


Fig. 6. Distribution of errors pre and post meta-optimization. Left panel: ground truth binding rate on the test set from grid 162-ieee-dtc (using 10k samples). Middle and right panels: comparison of the false positive rate and true-negative rates respectively for pre and post meta-optimization. Constraints are filtered to those that appear at least 20% in the ground truth. Constraint ordering is the same in each subplot.

larger grids we expect a much higher number of possibly binding constraints (Table II) and more significant difference of the meta-loss between the reduced OPF formulations and full model that reduce the possibility of the appearance of these trivial minima. To avoid the above pathological behaviour we introduced the penalty term discussed in Section-II-E4. This strategy resulted in a meta-loss-sensitive classifier (Figure 6).

The average gains of the meta-loss with two side 95% confidence intervals using 10 independent runs before and after the meta-optimization are collected in Table V. Gains are computed on the corresponding test sets relative to the meta-loss of the full OPF models as Eq 1 with  $t_f = \sum_{i=1}^{N_{\text{test}}} t_f^i$  and  $t_{\text{ML}} = \sum_{i=1}^{N_{\text{test}}} t_{\text{ML}}^i$ .

For DC-OPF cases we carried out experiments using 10k and 1k samples. Using 10k samples for 118-ieee, conventional optimization already results in a gain (38.2%) that was improved only slightly by meta-optimization. Given the limited number of distinct active sets (122) this training data size seems to be sufficient to obtain a fairly good classifier using the conventional loss. However, as the grid size increases, the gain provided by conventional training becomes drastically worse, resulting in poorer performance compare to that of the full problem. For each case, meta-optimization was able to improve the meta-loss significantly and bring the gain into the positive regime. To demonstrate how the meta-optimization works for very limited number of samples, where conventional training of the classifier would fail, we performed the above experiments using only 1k samples total. As expected, the gains after conventional optimization are very poor compared to the experiments with 10k samples. Using meta-optimization, however, provides an even larger improvement of the gains, indicating that even from this limited information the classifier can be optimized further with an appropriate objective function.

Finally, AC-OPF cases for 3 grids were also investigated using 1k samples. As the system sizes are much larger than their DC counterparts, it is not surprising that conventional training resulted in a poor gain for all cases. Meta-optimization again was able to improve all of them into the positive regime.

#### F. Improving the Initial State of Meta-optimization

Given the importance of a good initialization for meta-optimization we investigated whether further improvement can

TABLE V  
AVERAGE GAIN DURING META-OPTIMIZATION.

| Case         | Form | Gain (%)        |                 |                  |                 |
|--------------|------|-----------------|-----------------|------------------|-----------------|
|              |      | 10k             |                 | 1k               |                 |
|              |      | Pre             | Post            | Pre              | Post            |
| 118-ieee     | DC   | $38.2 \pm 0.8$  | $42.1 \pm 2.7$  | $13.9 \pm 2.1$   | $39.2 \pm 1.8$  |
| 162-ieee-dtc | DC   | $8.9 \pm 0.9$   | $31.2 \pm 1.3$  | $-12.4 \pm 2.3$  | $21.1 \pm 3.7$  |
| 300-ieee     | DC   | $-47.1 \pm 0.5$ | $11.8 \pm 5.2$  | $-73.3 \pm 1.7$  | $-4.7 \pm 9.4$  |
| 588-sdet     | DC   | $-56.0 \pm 0.5$ | $11.9 \pm 9.2$  | $-84.4 \pm 2.8$  | $-4.4 \pm 5.8$  |
| 1354-pegase  | DC   | $-94.6 \pm 2.8$ | $-27.8 \pm 4.7$ | $-123.2 \pm 8.8$ | $-33.8 \pm 6.0$ |
| 118-ieee     | AC   | —               | —               | $-33.1 \pm 2.9$  | $15.8 \pm 3.9$  |
| 162-ieee-dtc | AC   | —               | —               | $-61.9 \pm 7.3$  | $0.51 \pm 8.3$  |
| 300-ieee     | AC   | —               | —               | $-60.2 \pm 3.4$  | $-9.4 \pm 8.1$  |

be attained if the NN weights are initialized at a point closer to a local minimum of the meta-loss. Moreover, treating the conventional objective as a surrogate objective [28] for the meta-loss, we investigated if it can be modified to better represent this. For example, we can use a weighted cross-entropy loss that introduces an asymmetry between the false negative and false positive penalty terms:

$$-y \log(\hat{y})w - (1 - y) \log(1 - \hat{y})(1 - w), \quad (2)$$

where  $\hat{y} \in [0, 1]$  is the predicted probability of an arbitrary constraint's binding status,  $y \in \{0, 1\}$  is the ground truth, and  $w \in [0, 1]$  is the weight (note that a value of 0.5 corresponds to the unweighted classical cross-entropy). As we observed earlier, the meta-loss is much more sensitive to false negative predictions (Figure 4). To express this in the weighted cross-entropy expression we used  $w = 0.75$  and performed DC-OPF experiments as before using 10k samples (using the same setup for meta-optimization). The results are collected in Table VI. With this modification the gain was improved significantly compared to the conventional cross-entropy, and the corresponding meta-optimization also resulted in further improvement, outperforming the previous results.

Finally, we note that an even more representative loss function can be constructed by using individual weights for each constraint. These weights can then be optimized as hyperparameters using the meta-loss as the optimization target through a similar PSO framework. However, our preliminary experiments for DC-OPF showed that although there is a further reduction of the meta-loss, it still required a subsequent meta-optimization of the NN to have competitive performance to the above results. This suggests that under this parameterization of the classical objective, although the meta-loss can be minimized to a limited extent, in order to achieve further improvement a direct meta-optimization of the NN is needed. We leave a more thorough exploration to future work.

#### IV. CONCLUSION

A promising approach to reduce the computational time of solving OPF problems is to solve a reduced formulation, which is a considerably smaller problem. By training models offline, predictions of the active constraint set based on the real-time grid parameters can be performed with negligible cost. However, possible false negative predictions and the potential subsequent violation of the corresponding constraints can lead to infeasible solutions of the original (full) problem. This can

TABLE VI

AVERAGE GAIN OF META-OPTIMIZATION USING CONVENTIONAL AND WEIGHTED BINARY CROSS-ENTROPY WITH 10K SAMPLES AND DC-OPF.

| Case         | Gain (%)     |             |             |            |
|--------------|--------------|-------------|-------------|------------|
|              | Conventional |             | Weighted    |            |
|              | Pre          | Post        | Pre         | Post       |
| 118-ieee     | 38.2 ± 0.8   | 42.1 ± 2.7  | 43.0 ± 0.5  | 44.8 ± 1.2 |
| 162-ieee-dtc | 8.9 ± 0.9    | 31.2 ± 1.3  | 21.2 ± 0.7  | 36.9 ± 1.0 |
| 300-ieee     | -47.1 ± 0.5  | 11.8 ± 5.2  | -10.2 ± 0.8 | 23.2 ± 1.8 |
| 588-sdet     | -56.0 ± 0.5  | 11.9 ± 9.2  | -11.8 ± 1.0 | 24.6 ± 2.0 |
| 1354-pegase  | -97.1 ± 3.8  | -30.0 ± 4.5 | -54.9 ± 2.4 | -9.9 ± 5.4 |

easily appear for large grids, which have a significant number of distinct active sets.

This issue can be resolved by the iterative feasibility test used by certain grid operators. In this procedure, the solution of a reduced OPF problem is tested against all constraints of the full problem, the active set is extended by constraints that are violated, and a new reduced OPF problem is constructed and solved. The iteration is then terminated when no new constraint is violated, guaranteeing a solution of the full OPF problem.

In this paper we introduced a method for predicting active sets of constraints of OPF problems using neural network based classifiers and meta-optimization. The key ingredient of our approach is to replace the conventional loss function with an objective that measures the computational cost of the iterative feasibility test. This meta-loss function is then optimized by varying the weights of the NN.

For various synthetic grids, using DC- and AC-OPF formulations we demonstrated that NN classifiers optimized by meta-optimization resulted in a significantly shorter solve time of the iterative feasibility test than those of conventional loss optimization. Further, for several DC-OPF cases the meta-loss as optimized by meta-optimization outperformed that of the full OPF problem. For AC-OPF the performance was more moderate due to the large number of non-convex equality constraints, which are responsible for the majority of the computational cost of the OPF calculation. When comparing the performance for different grid sizes, meta-optimization appears to be an increasingly important component in identifying reduced formulations of OPF problems for larger grids.

Finally, we found that cross-entropy objective can be modified to obtain an improved meta-loss after conventional training, by weighting the contribution of the two types of classification errors. However, particularly for larger-grids, this meta-loss is still higher than that obtained after meta-optimization of the NN parameters directly, indicating that the conventional classification objective is insufficient to capture the meta-loss. Nevertheless, these approaches can be straightforwardly used as initialization step for meta-optimization.

## REFERENCES

- [1] J. Tong, "Overview of PJM energy market design, operation and experience," in *2004 IEEE International Conference on Electric Utility Deregulation, Restructuring and Power Technologies. Proceedings*, vol. 1. IEEE, 2004, pp. 24–27.
- [2] M. B. Cain, R. P. O'Neill, and A. Castillo, "History of optimal power flow and formulations," *Federal Energy Regulatory Commission*, vol. 1, pp. 1–36, 2012.
- [3] D. L. M. C. Data, "Nerc reliability guideline, draft, september, 2018."
- [4] A. V. Fiacco and G. P. McCormick, *Nonlinear Programming: Sequential Unconstrained Minimization Techniques*. New York, NY, USA: John Wiley & Sons, 1968, reprinted by SIAM Publications in 1990.
- [5] A. Wächter and L. T. Biegler, "On the implementation of a primal-dual interior point filter line search algorithm for large-scale nonlinear programming," *Mathematical Programming*, vol. 106, no. 1, pp. 25–57, 2006.
- [6] N. Guha, Z. Wang, and A. Majumdar, "Machine learning for AC optimal power flow." ICML, Climate Change: How Can AI Help? Workshop, 2019.
- [7] F. Fioretto, T. W. K. Mak, and P. Van Hentenryck, "Predicting AC Optimal Power Flows: Combining Deep Learning and Lagrangian Dual Methods," *arXiv e-prints*, p. arXiv:1909.10461, Sep 2019.
- [8] M. Jamei, L. Mones, A. Robson, L. White, J. Requeima, and C. Ududec, "Meta-optimization of optimal power flow." ICML, Climate Change: How Can AI Help? Workshop, 2019.
- [9] Q. Zhou, L. Tesfatsion, and C. Liu, "Short-term congestion forecasting in wholesale power markets," *IEEE Transactions on Power Systems*, vol. 26, no. 4, pp. 2185–2196, Nov 2011.
- [10] S. Misra, L. Roald, and Y. Ng, "Learning for Constrained Optimization: Identifying Optimal Active Constraint Sets," *arXiv e-prints*, p. arXiv:1802.09639, Feb 2018.
- [11] D. Deka and S. Misra, "Learning for DC-OPF: Classifying active sets using neural nets," *arXiv e-prints*, p. arXiv:1902.05607, Feb 2019.
- [12] X. Ma, H. Song, M. Hong, J. Wan, Y. Chen, and E. Zak, "The security-constrained commitment and dispatch for Midwest ISO day-ahead co-optimized energy and ancillary service market," in *2009 IEEE Power & Energy Society General Meeting*. IEEE, 2009, pp. 1–8.
- [13] Y. Ng, S. Misra, L. A. Roald, and S. Backhaus, "Statistical Learning For DC Optimal Power Flow," *arXiv e-prints*, p. arXiv:1801.07809, Jan 2018.
- [14] C. M. Bishop, *Pattern Recognition and Machine Learning (Information Science and Statistics)*. Berlin, Heidelberg: Springer-Verlag, 2006.
- [15] L. Mones, C. Ortner, and G. Csányi, "Preconditioners for the geometry optimisation and saddle point search of molecular systems," *Scientific Reports*, vol. 8, no. 1, p. 13991, 2018.
- [16] J. Kennedy and R. Eberhart, "Particle swarm optimization," in *Proceedings of ICNN'95 - International Conference on Neural Networks*, vol. 4, Nov 1995, pp. 1942–1948 vol.4.
- [17] S. Babaeinejadsarookolae, A. Birchfield, R. D. Christie, C. Coffrin, C. DeMarco, R. Diao, M. Ferris, S. Fliscounakis, S. Greene, R. Huang, C. Jozs, R. Korab, B. Lesieutre, J. Maeght, D. K. Molzahn, T. J. Overbye, P. Panciatici, B. Park, J. Snodgrass, and R. Zimmerman, "The Power Grid Library for Benchmarking AC Optimal Power Flow Algorithms," *arXiv e-prints*, p. arXiv:1908.02788, Aug 2019.
- [18] C. Coffrin, R. Bent, K. Sundar, Y. Ng, and M. Lubin, "PowerModels.jl: An open-source framework for exploring power flow formulations," in *2018 Power Systems Computation Conference (PSCC)*. IEEE, 2018, pp. 1–8.
- [19] J. Bezanson, S. Karpinski, V. B. Shah, and A. Edelman, "Julia: A fast dynamic language for technical computing," *arXiv preprint arXiv:1209.5145*, 2012.
- [20] A. Domahidi, E. Chu, and S. Boyd, "ECOS: An SOCP solver for embedded systems," in *2013 European Control Conference (ECC)*. IEEE, 2013, pp. 3071–3076.
- [21] B. Stellato, G. Banjac, P. Goulart, A. Bemporad, and S. Boyd, "OSQP: An operator splitting solver for quadratic programs," *ArXiv e-prints*, Nov. 2017.
- [22] M. Innes, "Flux: Elegant machine learning with Julia," *J. Open Source Software*, vol. 3, no. 25, p. 602, 2018.
- [23] S. Ioffe and C. Szegedy, "Batch normalization: accelerating deep network training by reducing internal covariate shift." ICML, 2015.
- [24] V. Nair and G. E. Hinton, "Rectified linear units improve restricted boltzmann machines." ICML, 2010.
- [25] N. Srivastava, G. Hinton, A. Krizhevsky, I. Sutskever, and R. Salakhutdinov, "Dropout: A simple way to prevent neural networks from overfitting." *JMLR*, 2014.
- [26] D. P. Kingma and J. Ba, "Adam: A method for stochastic optimization," *arXiv preprint arXiv:1412.6980*, 2014.
- [27] P. K. Mogensen and A. N. Riseth, "Optim: A mathematical optimization package for Julia," *Journal of Open Source Software*, vol. 3, no. 24, p. 615, 2018.
- [28] I. Goodfellow, Y. Bengio, and A. Courville, *Deep Learning*. MIT Press, 2016.